

MODELING SEASONAL HYDRODYNAMIC REGIMES AND THEIR ROLE IN SHAPING MEGA CUSPS: INSIGHTS FROM MY KHE BEACH, VIETNAM

Authors: Nguyen Quang Duc Anh¹, Dinh Nhat Quang², Nguyen Truong Duy¹, Hitoshi Takana³, Abdelkader Hammouti⁴, Damien Pham Van Bang^{4,*}, Nguyen Trung Viet²

1 Institute of Civil Engineering, Thuyloi University, Hanoi, Vietnam;

2 Department of Civil Engineering, Thuyloi University, Hanoi, Vietnam;

3 Institute of Liberal Arts and Sciences, Tohoku University, Sendai, Japan;

4 Department of Construction Engineering, École de Technologie Supérieure, Université du Québec, Montréal, Canada;

* corresponding author: damien.pham-van-bang@etsmtl.ca

Abstract

This study examines seasonal hydrodynamics shaping coastal morphology at My Khe Beach, Vietnam, with emphasis on mega cusp formation and evolution. A calibrated Delft3D model simulated wave fields, nearshore circulation, and processes using satellite, AUV, bathymetric, tidal, wave, and current data from field campaigns conducted in January and May 2024. The simulations reproduce the seasonal variability in coastal dynamics with reasonable accuracy. During the northeast monsoon, ENE and NE waves with significant heights (Hs) of 1.5–2.0 m generated strong nearshore currents that intensified beach erosion and promoted mega cusp formation. In contrast, during the southwest monsoon, ESE and SE waves with Hs around 1.0 m and oblique incidence angles reduced nearshore flow velocities ($V < 0.2$ m/s), mitigating erosional processes and contributing to beach profile stabilization. Results emphasize seasonal wave forcing as a key driver of coastal morphology and present a robust modeling framework to support management in monsoon-influenced regions.

Keywords: coastal erosion, mega cusp, hydrodynamic modeling, monsoon waves, Delft3D

1. Introduction

Coastal erosion and shoreline instability pose significant challenges worldwide, exacerbated by global climate change, socio-economic development, and increasing tourism pressures. Understanding and integrating coastal morphodynamics - the dynamic interaction between waves, currents, sediment transport, and shoreline evolution - is essential for sustainable coastal planning and management. As climate change accelerates sea-level rise and intensifies storm events, many coastal systems become increasingly vulnerable to erosion, flooding, and habitat loss (Clark, 1997; Martínez et al., 2011). This vulnerability is particularly critical in rapidly developing coastal regions, where infrastructure and livelihoods are directly exposed to shoreline instability. Aligning coastal development with the natural behavior of sedimentary systems can reduce long-term risks and promote sustainable interactions between human and natural systems.

Global climate models predict an increase in the frequency and intensity of extreme coastal events, while concurrent expansion of urbanized coastal zones amplifies both exposure and vulnerability, escalating overall coastal risk (IPCC, 2023; Kulp & Strauss, 2019). Southeast Asia exemplifies this trend, identified as a global hotspot for coastal hazards due to its dense

49 coastal populations, rapid urban development, and high dependence on marine-based
50 economies (Vila-Concejo et al., 2024; Hue et al., 2020).

51 Effective coastal adaptation strategies must be tailored to the specific hydrodynamic forcing,
52 sedimentary regimes, and socio-economic contexts of each site. Recent studies emphasize
53 combining hydrodynamic modeling, morphological forecasting, and stakeholder engagement
54 to identify optimal trade-offs between protection, conservation, and development (Morales,
55 2022; Chowdhury et al., 2023). Such site-specific approaches are essential for designing
56 sustainable interventions that align with both natural coastal dynamics and long-term human
57 interests.

58 Mega cusp beaches are prominent rhythmic shoreline features characterized by large-scale
59 embayments alternating with protruding cusp horns, typically spaced hundreds of meters apart
60 (e.g., Thornton et al., 2007; Short & Masselink, 1992). These features are formed through the
61 interaction of waves and nearshore currents, often associated with standing edge-wave patterns
62 or rip current cells. Unlike depositional features such as spits or tombolos, mega cusp beaches
63 accentuate shoreline rhythmicity through their embayment-cusp system and are highly sensitive
64 to variations in hydrodynamic forcing. Their well-defined cusp patterns play a critical role in
65 sediment redistribution, with erosion typically concentrated in the embayments and deposition
66 occurring at the cusp tips.

67 The formation and evolution of mega cusp beaches are shaped by both natural processes and
68 human activities. In monsoon-dominated regions such as Southeast Asia, seasonal wave
69 regimes exert a strong control on coastal morphodynamics. During the northeast monsoon,
70 energetic waves and enhanced rip-current circulation intensify cross-shore sediment transport,
71 which accentuates and maintains cusp embayments. In contrast, the calmer southwest monsoon
72 favours onshore sediment transport and partial infilling of embayments, smoothing the cusp
73 morphology (Thanh et al., 2018). These alternating conditions create a cyclical pattern of
74 erosion and recovery that is critical for understanding shoreline stability.

75 The dominant hydrodynamic regime (whether wave-dominated, tide-dominated, or mixed)
76 also shapes the morphodynamic response of the coast. Wave-dominated systems are typically
77 characterized by strong longshore currents and bar-trough morphologies, while tide-dominated
78 systems exhibit broader intertidal zones and more uniform sediment transport patterns.

79 A key parameter in sediment transport and morphological change is bed shear stress, which
80 quantifies the force exerted by fluid flow on the seabed (Nielsen, 1992). When this stress
81 exceeds a critical threshold, sediment is mobilized, leading to erosion or redistribution.
82 Seasonal variations in wave height and direction significantly influence bed shear stress,
83 particularly during storm events or monsoonal transitions.

84 Longshore currents and rip currents are also fundamental components of nearshore
85 circulation, each playing a critical role in sediment transport and the development of cusped
86 shoreline features (Wright & Short, 1984). Longshore currents, generated by waves
87 approaching the coast at an oblique angle, redistribute sediment parallel to the shoreline and
88 drive progressive shoreline change. In contrast, rip currents - narrow, seaward-directed flows
89 often concentrated in low points or embayments - export sediment offshore, deepening
90 embayments and influencing cusp spacing (Guza & Inman, 1975; Castelle et al., 2016). The
91 interaction between these two current systems and the pre-existing beach morphology
92 establishes feedback mechanisms that can either stabilize rhythmic shoreline features under
93 steady forcing or destabilize them during storms and changing wave regimes.

94 Recent advances in sediment tracing, particularly the application of radionuclide mapping, have
95 expanded the capacity to identify deposition and erosion zones along dynamic coastlines. By
96 capturing fine-scale spatial patterns of sediment redistribution, this method provides a robust
97 tool for diagnosing coastal processes. Its utility is most evident in environments with contrasting
98 wave exposure, where sheltered and exposed zones can be clearly distinguished (Tsabaris et
99 al., 2025).

100

101 My Khe Beach, on the eastern coast of Da Nang, is a major tourist destination and key regional
102 asset, yet it is highly dynamic due to its moderate tidal range (~1.2 m) and strong seasonal wave
103 forcing. Situated between the Cua Dai estuary and the Son Tra Peninsula, it exhibits mixed tidal
104 and wave-driven processes that generate distinctive mega cusps—shoreline features with 100–
105 300 m spacing and up to 50 m radii—forming under northeast monsoon conditions and
106 dissipating during the calmer southwest monsoon. Despite its socio-economic importance, the
107 beach has suffered recurrent erosion, notably in December 2017, with satellite imagery showing
108 scouring concentrated in cusp embayments. While previous studies (Viet et al., 2015; Tanaka
109 et al., 2016, 2017; Tinh et al., 2018) underscored the need for detailed analysis, site-specific
110 investigations of the hydrodynamic drivers remain limited. This study addresses that gap by
111 numerically simulating seasonal regimes governing the formation and evolution of mega cusps
112 at My Khe Beach (Figure 1).

113 Remote sensing data analysis has indicated that the formation of large mega cusps is one
114 of the primary factors driving erosion at My Khe Beach (Viet et al., 2018). Satellite imagery
115 analysis shows that the alongshore spacing (λ) of these features ranges from 100 to 300 meters,
116 with cusp radii (h) reaching up to approximately 50 meters, clearly reflecting the influence of
117 wave dynamics on beach morphology in this area (Figure 1). These cusped formations result
118 from the complex interaction between wave action and coastal currents, where prolonged high-
119 energy wave conditions alter sediment transport dynamics and coastal topography, with erosion
120 concentrated in the embayments where sediment removal is most intense (Thornton et al. 2007).

121 Understanding coupled hydrodynamic and sedimentary processes is critical for studying
122 mega cusps, which serve as natural laboratories for assessing coastal vulnerability and
123 resilience. On rapidly urbanizing shorelines such as Da Nang, where infrastructure and tourism
124 are highly exposed, these insights directly inform adaptive coastal management. Accounting
125 for seasonal seabed dynamics is essential, as process-based approaches offer greater resilience
126 to anthropogenic pressures and climate change. Site-specific approaches are particularly
127 important to ensure sustainable interventions that align with coastal morphodynamics, as
128 interactions between current systems and beach morphology can either stabilize or destabilize
129 rhythmic shoreline features under varying wave regimes and storm events.

130 The objective of this study is to simulate the hydrodynamic regimes and morphological
131 changes in the My Khe beach area; the collection of input data is of paramount importance to
132 ensure the accuracy and feasibility of the modeling process. For future sediment transport study,
133 this study presents for the first time a numerical model to simulate hydrodynamic regime on
134 My Khe beach to describe the asymmetric gain and loss of sediment, characterizes the long-
135 term irreversible tendency to erosion (Figure 1). This will serve in future to validate a
136 morphodynamic beach model and further design adaptation solution to minimize climate effects
137 on this region. This study focuses on the detailed simulation and analysis of hydrodynamic
138 factors to determine the relationship between wave dynamics, nearshore circulation, and the
139 occurrence of mega cusps erosion along the My Khe coastline.

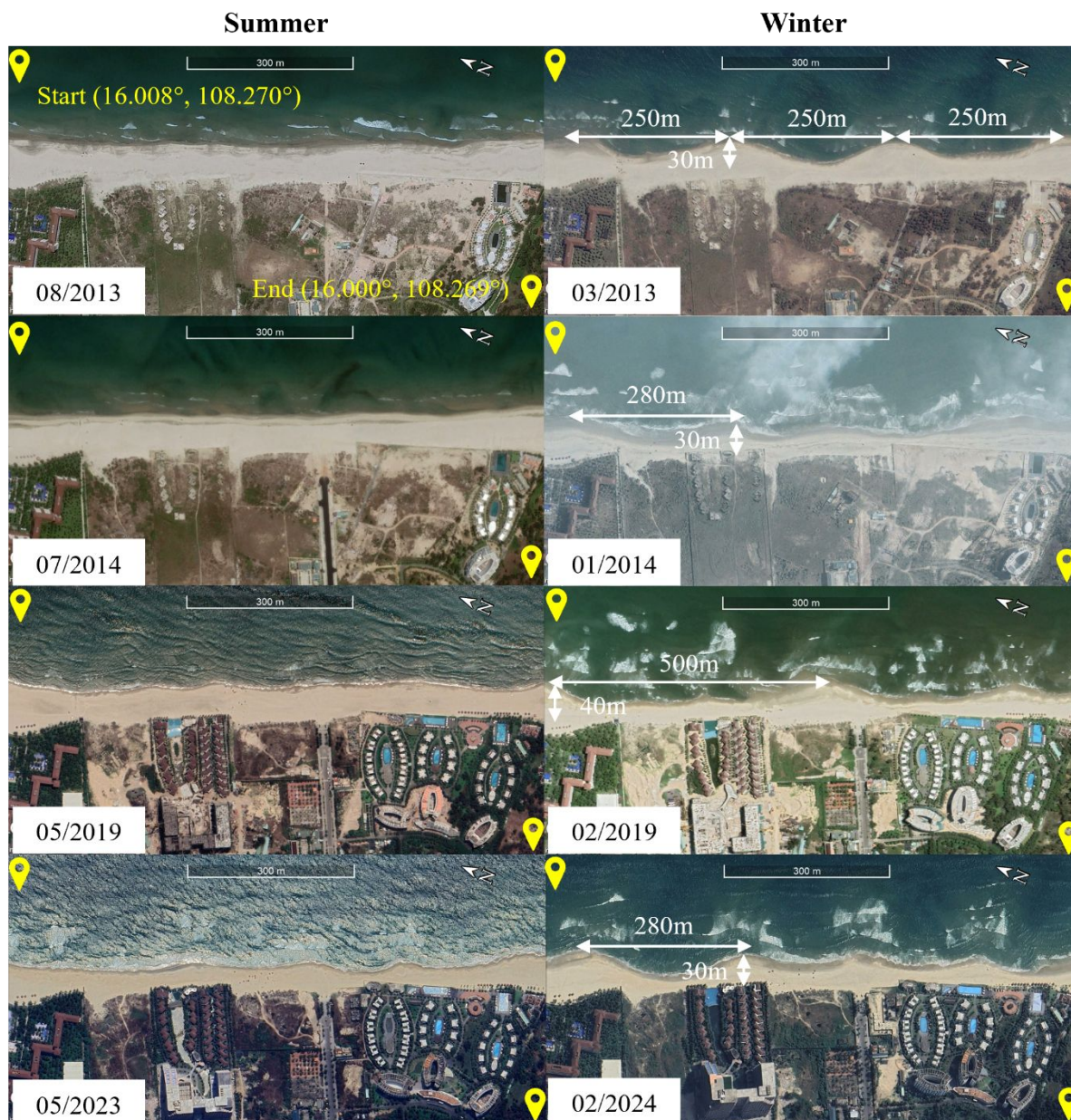


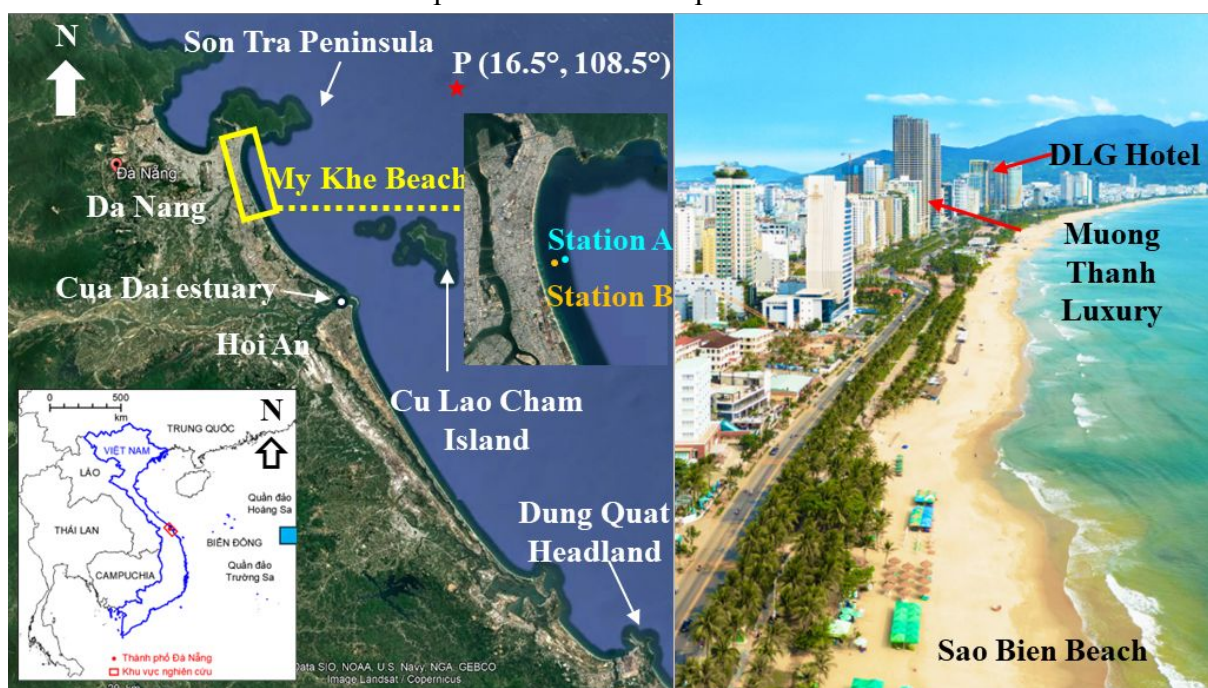
Fig. 1. The coastal morphology of My Khe Beach with the presence of a mega beach cusp (in winter) and its absence (in summer) with start/end GPS points. (Figure was created using Google Maps, version 2025 and assembled from the following data source: Research project 2022-2025 titled “*Development of a Toolset for Assessing and Forecasting Morphological Changes and Proposing Stabilization Solutions for Beaches in the Central Coastal Region of Vietnam*”.)

The structure of the paper is organized as follows: In Section 2, we introduce the study area and outline the methodology, including data collection and hydrodynamic modeling approaches. Section 3 presents the results of the numerical simulations, focusing on wave dynamics, nearshore currents, and bed shear stress under seasonal monsoon conditions. Finally, Section 4 provides a discussion of the findings, highlighting the influence of monsoonal variability on coastal morphodynamics and addressing the limitations of the study.

2. Site and methodology

156 2.1 Study site: My Khe beach

157 My Khe Beach, located on the eastern coast of Da Nang, is renowned for its white sandy
 158 shores, clear blue waters, and mild climate. With its favorable geographical position -bordered
 159 by the Cua Dai estuary to the south and the Son Tra Peninsula to the north - My Khe plays a
 160 vital role in the development of the Central Region's marine economy, particularly in tourism
 161 and services. However, over the past decade, the beach has been facing severe erosion, causing
 162 significant damage to coastal infrastructure. This issue has been observed since 2017, especially
 163 in the area stretching from the My Khe drainage outlet to the Premier Village resort, and most
 164 recently in January 2025, when erosion at the My Khe bathing area led to the destruction of
 165 several structures (Figure 2). Satellite imagery shows mega beach cusps with 100–300 m
 166 spacing and ~50 m curvature radii, where erosion concentrates in embayments. MBES-derived
 167 DEM differencing over 5 km (January 2024–2025) reveals a net nearshore sediment loss of
 168 $\sim 1.17 \times 10^6 \text{ m}^3$. Bed lowering dominates within 200–250 m of the shoreline, with partial
 169 redistribution 300–450 m offshore, while morphodynamic adjustments remain mainly within
 170 the inner 500 m and sediment displacement extends up to ~400 m offshore.



171
 172 **Fig. 2.** My Khe beach, Da Nang (Vietnam) and Cua Dai estuary between Son Tra Peninsula
 173 and Dung Quat headland. Waves data at Point P at 100m depth, Station A (16,048°; 108.256°)
 174 at 12m depth and B (16.051°; 108.268°) at 6m depth for waves and currents measured by
 175 AWAC equipment (Figure was created using Google Maps, version 2025 and assembled from
 176 the following data source: Research project 2022-2025 titled “*Development of a Toolset for*
 177 *Assessing and Forecasting Morphological Changes and Proposing Stabilization Solutions for*
 178 *Beaches in the Central Coastal Region of Vietnam*”).

179

180

181 The beach frequently exhibits mega cusps erosion, a geomorphological feature shaped by the
 182 interaction of waves and nearshore currents, where the shoreline takes on a sawtooth-like
 183 pattern. During periods of strong wave activity, sediments are transported offshore, forming
 184 submerged sandbars, while weaker wave conditions promote sediment deposition and the
 185 development of large mega cusps features, particularly during the northeast monsoon season.
 186 Erosion primarily occurs in the embayments between the cusps, where sediment is most
 187 intensely scoured (Việt et al., 2018). In contrast, during the southwest monsoon season, when
 188 wave energy is lower, these cusped features gradually flatten and reshape, contributing to
 189 shoreline stabilization.

190

191 Shoreline positions were extracted using a multi-platform monitoring framework that
 192 integrates satellite remote sensing and UAV photogrammetry. Multi-decadal shoreline
 193 dynamics were reconstructed from the Landsat series (5 TM, 7 ETM+, 8/9 OLI/TIRS; 30 m
 194 spatial resolution, 16-day revisit) for the period January 1990–December 2024, and from
 195 Sentinel-2 MSI for the period June 2015– December 2024 (10–20 m spatial resolution, 5-day
 196 revisit) for the period 1990–2024. These satellite datasets, processed with the CoastSat toolbox
 197 and corrected for tidal stage, provided a consistent synoptic record for quantifying long-term
 198 erosion and accretion patterns along the Da Nang coast. The extracted shorelines are subject to
 199 inherent uncertainties from sensor resolution and geolocation, cloud/sun-glint and wave foam,
 200 and CoastSat's automated classification.

201 To capture finer-scale variability, UAV surveys were conducted between 2022 and 2024 at
 202 My Khe Beach. The surveys produced orthomosaics and high-resolution digital elevation
 203 models with ground sampling distances of 2–5 cm, which were validated against RTK-GNSS
 204 ground control points and in-situ beach profiles. Together, the integration of these observation
 205 systems established a nested, multi-scale dataset: satellites for multi-decadal trends and UAVs
 206 for seasonal to interannual dynamics

207

208

2.2 Data Collection and Input Parameters

209

210

211

212

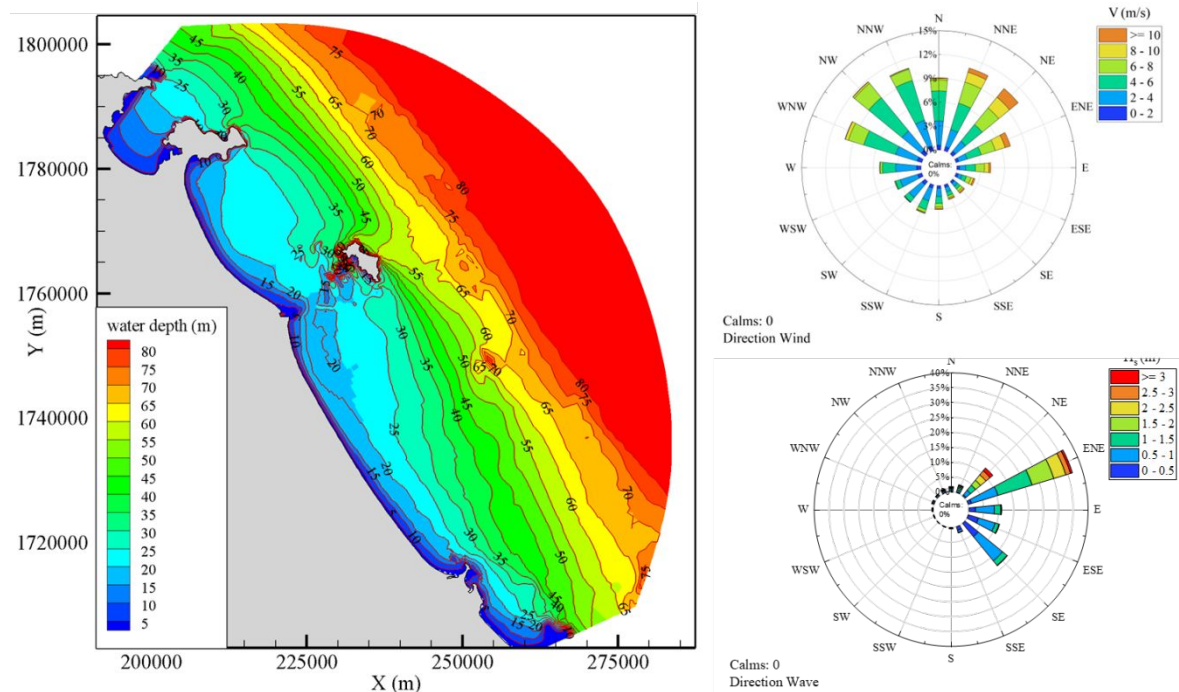
213

214

215

To simulate the hydrodynamic regimes and morphological changes in the My Khe beach
 area, the collection of input data is of paramount importance to ensure the accuracy and
 feasibility of the modeling process. The dataset used in this study was obtained from the
 research project 2022-2025 titled "*Development of a Toolset for Assessing and Forecasting
 Morphological Changes and Proposing Stabilization Solutions for Beaches in the Central
 Coastal Region of Vietnam*".

216



216

217

218

Fig 3. Site data and offshore forcing statistics for My Khe Beach (Da Nang, Vietnam): bathymetry (left); wind rose from NCEP–NOAA 10-m winds (U_{10}, V_{10}) at point P (top-right);

219 wave rose from WAVEWATCH III based on Station A and B (bottom-right).

220

221 2.2.1. Bathymetry data

222 The dataset comprises several topographic and bathymetric mapping products to
223 characterize both terrestrial and underwater zones of the My Khe beach area and its broader
224 coastal region. A detailed topographic survey map of the My Khe beach terrestrial zone was
225 prepared at a fine scale of 1:500, with contour intervals of 0.5 meters. This high-resolution map
226 provides precise elevation data essential for understanding landform features and coastal slope
227 gradients. For the adjacent submerged zone, a bathymetric map was produced at a scale of
228 1:2000, featuring 1.0-meter contour intervals to capture the underwater terrain with adequate
229 detail for coastal process modeling. These smaller-scale maps allow for detailed analysis of
230 shoreline changes and nearshore morphology.

231 To extend the spatial context beyond the immediate beach zone, a broader regional coastal
232 bathymetric map covering the coastline from Quang Nam to Quang Binh provinces was also
233 incorporated. This map, originally surveyed by the U.S. Navy in 1970, is at a scale of 1:50,000
234 with 20-meter contour intervals. Although coarser in resolution, it offers critical information on
235 offshore bathymetry and seabed gradients influential to sediment transport and wave dynamics
236 on a regional scale. Additionally, global bathymetric grid data from the General Bathymetric
237 Chart of the Oceans (GEBCO) were utilized to supplement regional assessments and provide a
238 comprehensive overview of underwater topography extending offshore (Figure 3).

239 Together, these multi-scale datasets enable integration from fine local terrain and seabed
240 features to broader regional slopes and depths, facilitating a detailed understanding of coastal
241 and nearshore morphodynamics at My Khe and its surrounding coastal waters.

242

243 2.2.2. Hydrodynamic data

244 Tidal boundary conditions for this study were extracted from the TPXO7.0 global tidal model
245 (Egbert and Erofeeva, 2002). The amplitudes of the principal tidal harmonic constituents (K1,
246 O1, M2, and S2) were determined to be 0.17 m, 0.11 m, 0.19 m, and 0.07 m respectively. Using
247 these harmonic amplitudes, yielding a tidal form factor $F=1.077$ (Pugh, 2004; Van Maren et
248 Gerritsen, 2012). This indicates a mixed tidal regime at My Khe Beach. While the semi-diurnal
249 M2 component exhibits the largest amplitude at 0.19 m, the diurnal constituents K1 and O1,
250 with amplitudes of 0.17 m and 0.11 m respectively, exert significant influence on the overall
251 tidal dynamics. According to tidal classification criteria, a form factor F value between 0.5 and
252 1.0 typically characterizes a mixed tide with a dominance of semi-diurnal components.
253 However, at My Khe Beach, with an F factor slightly above this range at 1.077, the tidal regime
254 is best described as mixed with a prevailing diurnal influence. This nuanced tidal character is
255 critically important for understanding and predicting tidal fluctuations, as it affects sediment
256 transport, coastal circulation patterns, and the morphology of coastal features such as mega
257 cusps. Accurately characterizing the tidal regime supports improved modeling of coastal
258 processes and informs management efforts aiming to mitigate environmental and anthropogenic
259 impacts in the region.

260 Wave climate data from 2000 to 2023 were extracted from the third-generation reanalysis wave
261 model WAVEWATCH III, developed by NOAA. Wind forcing was taken from the NCEP–
262 NOAA reanalysis as standard 10-m winds (U_{10} , V_{10}) over the sea surface (hourly; $0.2^\circ \times 0.2^\circ$;
263 2000–2024). Wind and wave time series were extracted at an offshore point P (16.5°N ,
264 108.5°E), approximately 100 km seaward of My Khe Beach (Figure 2), to derive the wind/wave

265 rose statistics (Figure 3) and to define offshore forcing. In addition, wave climate data were
266 measured at points A, B (Figure 2) using AWAC from 2020 to 2025. Finally, for the present
267 study aiming to develop and validate the coastal model for future sediment transport
268 assessment, the two recent field survey data were conducted in January and May 2024.
269 Measurements at stations A and B included water levels, wave parameters, and current
270 velocities, with survey periods spanning from January 16–23, 2024 (campaign 1, monsoon
271 winter or NorthEastern) and May 15–22, 2024 (campaign 2, monsoon summer SouthEastern).
272 The locations of these stations are illustrated in Figure 2.

273 Nearshore wave induced current are measured at point A, B using velocimetry sensor
274 (Nortek) during the same period January 16-23 and May 15-22, 2024. From measurements, it
275 is observed an intense longshore current from North to South during the winter (or ENE)
276 monsoon and a moderate current from south to North during the summer (or ESE) monsoon.

277 2.2.3. Shoreline data

278 The shoreline dataset at My Khe Beach provides an integrated record of morphological
279 variability spanning seasonal to interannual timescales (Figs. 4–5). Rather than exhibiting a
280 uniform trend, the shoreline demonstrates cyclic erosion and recovery patterns related to cusps
281 dynamics under alternating monsoon regimes. Significant shoreline retreat occurs within
282 embayment zones during the northeast monsoon (e.g., January 2017, 2024), whereas calmer
283 conditions in the summer months promote partial accretion and restoration of cusp morphology.

284 High-resolution bathymetric surveys conducted between 2024 and 2025 complement these
285 observations by revealing nearshore morphological features such as rip channels, submerged
286 bars, and offshore cusp extensions. These seabed structures exert strong control over sediment
287 circulation and transport pathways. The spatial correspondence between seabed morphology
288 and erosion hotspots underscores the close coupling between wave climate, cross-shore
289 sediment exchanges, and shoreline adjustment processes.

290 Collectively, this comprehensive dataset establishes a robust empirical baseline for linking
291 hydrodynamic forcing to morphodynamic responses, offering essential insights for future
292 sediment transport modeling and comparative studies of monsoon-dominated coastal systems.

293

294 **2.3 Hydrodynamic model**

295 The study on hydrodynamic regimes and sediment transport processes at My Khe Beach was
296 conducted using the Delft3D modeling suite developed by Deltares to provide insight into the
297 physical processes explaining the cyclicity in the formation of megacusp and their smoothing
298 during the ENE (winter) and ESE (summer) monsoon respectively.

299 For the coupling between tides and waves, two main modules are selected for computation
300 on a curvilinear orthogonal grid. On the one hand, Delft3D-Flow module solves the so-called
301 shallow water equation (SWE) assuming hydrostatic pressure and depth-integrated velocities.
302 On the other hand, Delft3D-Wave is used for wave propagation and interaction (Lesser et al.,
303 2004). The coupling between these two modules through radiation stresses enables the analysis
304 of wave–current interactions and gives access to the bed shear stresses which are crucial
305 parameter for future sediment transport study but are very difficult to assess in field conditions.
306

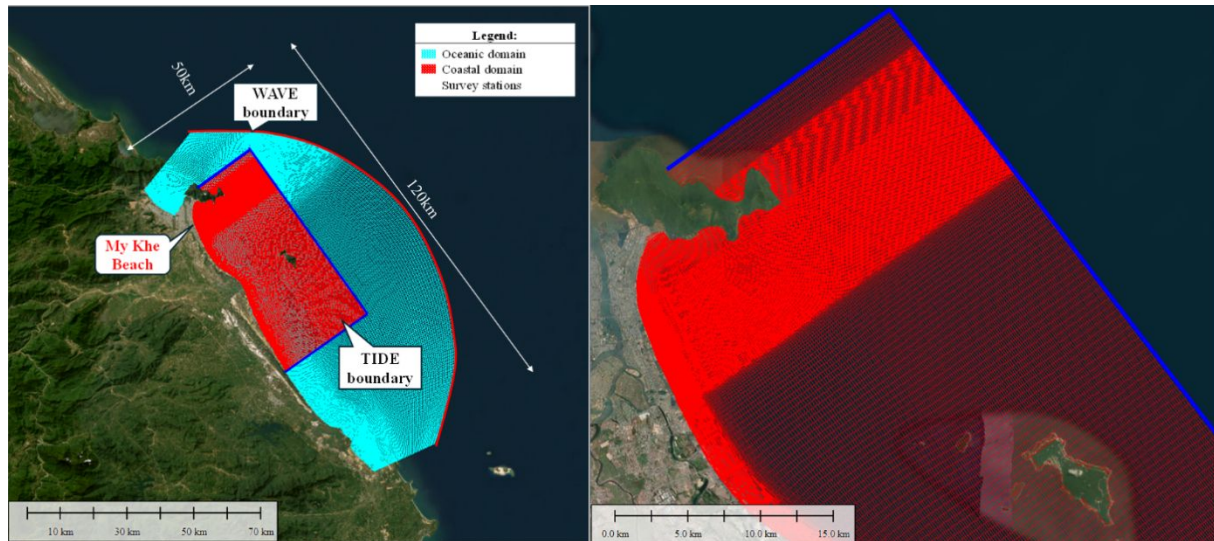
307 Figure 4 presents the extend of computational domain which is subdivided in two subdomains:

308 (i) The oceanic domain covers a zone of 120 x 50 km² to include the Son Tra Peninsula at the
309 northern limit and the Dung Quat Headland at the southern limit. The Wave boundary conditions
310 were derived from NOAA's WAVEWATCH III model at offshore point P.

311 (ii) The coastal domain covers a zone of 50 x 25 km² centered to the Cua Dai estuary and Cu Lao
312 Cham Island. The Tide boundary conditions were derived from the TPXO7.0 global tidal

313 model.

314



315

316 **Fig 4.** Computational domains and open boundaries : (1) oceanic domain for wave propagation
 317 with the offshore wave boundary (Delft3D-WAVE) forced by WAVEWATCH III at point P;
 318 and (2) coastal domain for tide-driven circulation with open-boundary water levels (Delft3D -
 319 FLOW) prescribed from TPXO7.0 tidal constituents. (Figure was created using Google Maps,
 320 version 2025 and assembled from the following data source: Research project 2022-2025 titled
 321 “Development of a Toolset for Assessing and Forecasting Morphological Changes and
 322 Proposing Stabilization Solutions for Beaches in the Central Coastal Region of Vietnam”.)

323

324 For Delft3D-FLOW, tidal water levels are implemented as harmonic forcing (data extracted
 325 from TPXO7.0 tidal constituents), and vary in time and along the open boundaries, i.e., not
 326 constant along the boundary line. For Delft3D-WAVE, the offshore wave boundary is uniform
 327 along the boundary, using a time series (data extracted from WAVEWATCH III at point P) for
 328 calibration/validation and stationary sea states for scenarios.

329

330 2.4 Model Calibration and Validation

331 The selection of model parameters is a crucial and complex process, carried out through
 332 multiple iterations of adjustment and testing to achieve accurate simulation results. These
 333 parameters include the model domain, grid size, time step, and physical parameters. Among
 334 these, determining the model domain and grid size is particularly important, especially in the
 335 nearshore region, where wave and flow dynamics vary significantly.

336

337

Table 1. Key model parameters for Flow and Wave Modules

Parameters	Flow Model	Parameters	Wave Model
Manning	0.026	gamma	0.73
Eddy viscosity	1 m ² /s	alpha	1
Dryflyc	0.05 m	Bottom friction	0.067 m ² /s ³
		Min. depth	0.05 m

338

339 This area is influenced by a variety of hydrodynamic and topographic factors, which require
 340 careful consideration of the model's extent and grid resolution. To accurately simulate processes
 341 in this region, the computational grid is set with 320 grid cells in the M direction, 500 grid cells
 342 in the N direction, and a minimum grid size of 30 m x 30 m for the coarse grid. For more
 343 detailed simulations, the fine grid is adjusted to 650 grid cells in the M direction, 500 grid cells

344 in the N direction, with a minimum grid size of 10 m x 10 m, ensuring higher resolution,
 345 especially in the shallow water areas and the time step is adjusted to 1 minute. These optimal
 346 resolution was based on a space–time convergence analysis, conducted by progressively
 347 refining the grid resolution from 50 m to 5 m and reducing the computational time step from 5
 348 min to 10 s. Based on these tests, a nested-grid configuration with a final time step of $\Delta t = 1$
 349 min was adopted as an optimal compromise between numerical stability and computational
 350 efficiency. The selected setup satisfies the CFL stability criterion throughout the domain.
 351 Details of the convergence strategy and its application are consistent with methodologies
 352 reported in Dien et al. (2019).

353

354 For the Delft3D-wave model, the default value of JONSWAP parameters were applied (Battjes
 355 and Janssen's model). The only adjustment concerned the wave rose discretization, using 36
 356 wave directions, each divided into 100 segments, with frequencies ranging from 0.05 Hz to 1
 357 Hz, and distributed over 24 frequency bands. For the Delft3D-Flow model, the only three
 358 parameters (Manning bottom friction, eddy viscosity and wet/dry threshold) were adjusted
 359 through calibration and verification. We consider here a constant eddy viscosity model. Table
 360 1 summarizes the parameter values obtained from the validation procedure.

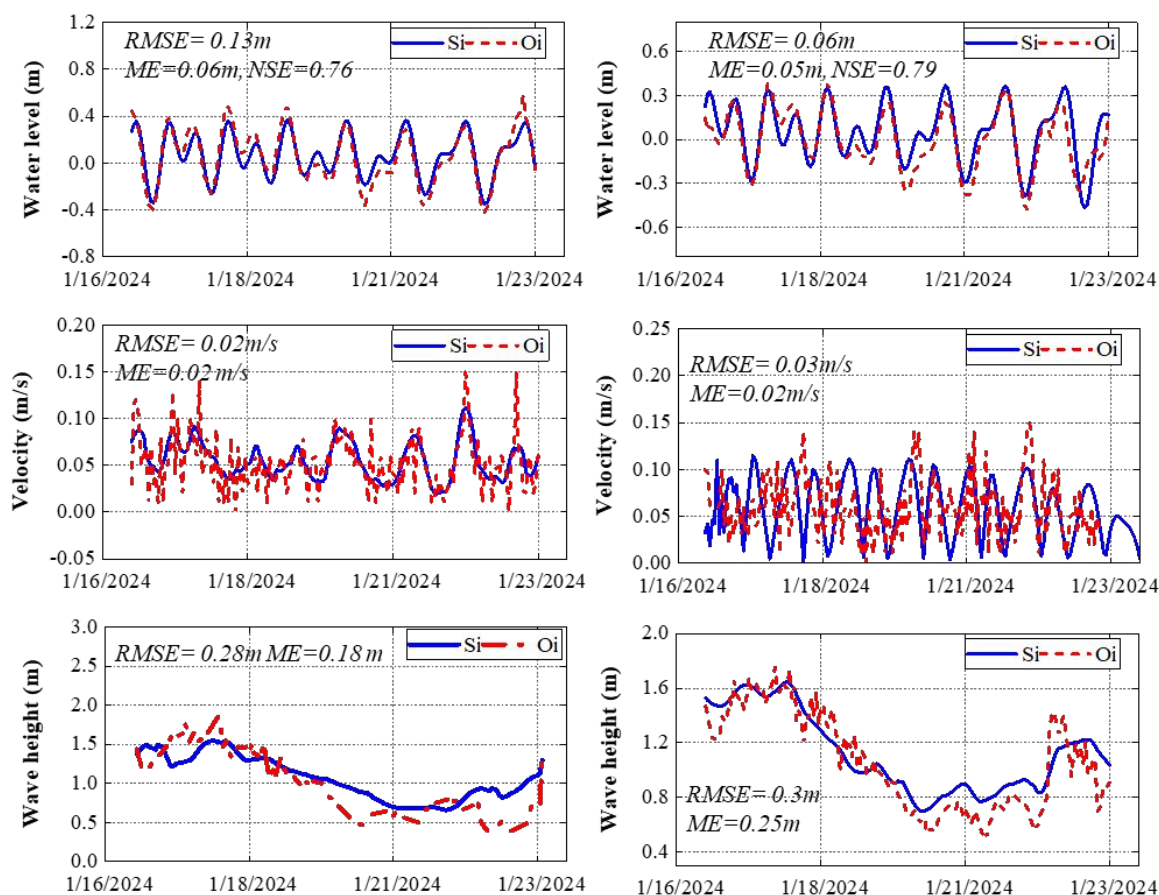
361 In this study, the model was calibrated and validated using field data collected in January
 362 and May 2024 at Stations A and B (Figure 2), located offshore of the My Khe Beach area.
 363 Water level, wave, and current velocity measurements from January 2024 were used for
 364 calibration, with parameters adjusted to minimize the Root Mean Square Error (RMSE) and
 365 Mean Error (ME), while maximizing the Nash–Sutcliffe Efficiency (NSE) coefficient
 366 (Williams & Esteves, 2017). Model accuracy was further verified through comparison with
 367 May 2024 observations. The calibration and verification processes ensured that simulated wave
 368 and flow dynamic are closely reproduced observed conditions, thereby improving confidence
 369 in the model's ability to represent natural processes within the study area.

370

$$371 \quad RMSE = \sqrt{\frac{1}{N} \sum_{i=1}^N (S_i - O_i)^2} \quad ME = \frac{1}{N} \sum_{i=1}^N |O_i - S_i| \quad NSE = 1 - \frac{\sum_{i=1}^N (S_i - O_i)^2}{\sum_{i=1}^N (O_i - \bar{O})^2}$$

372 where O_i stands for the observed value, S_i the simulated value, N the number of data points,
 373 and \bar{O} the mean of the observed data series.

374



375

376

Fig 5. Results of Calibration on water level, current, and wave parameters at Station A (left) and Station B (right) during the first (January 2024) survey campaign

377

378

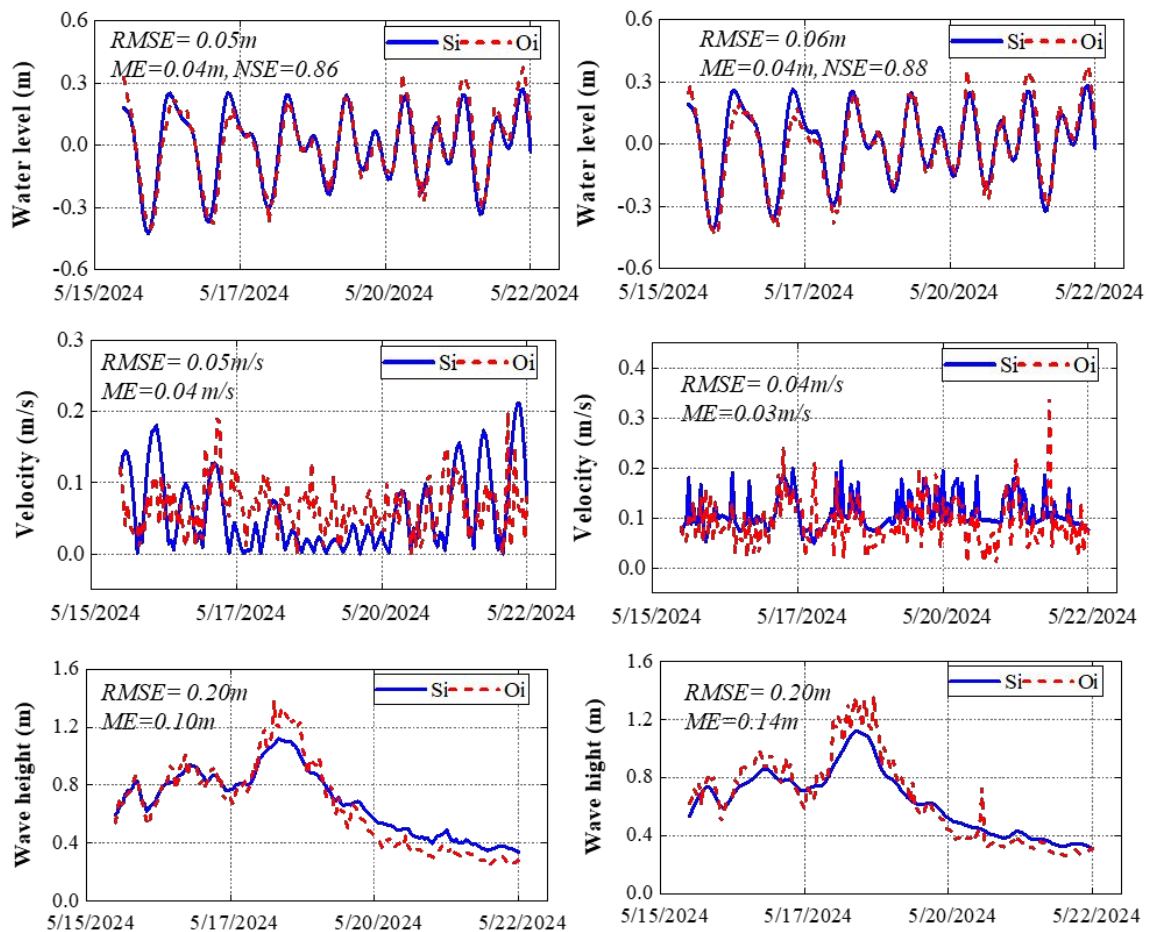
379 During calibration (Figure 5), water levels were reproduced with RMSE of 0.05–0.08 m and
 380 NSE of 0.76–0.79, while current velocity errors remained low (RMSE of 0.06–0.12 m/s).
 381 Significant wave height (H_s) showed RMSE of approximately 0.28–0.30 m under higher-
 382 energy winter conditions.

383 During verification against the May 2024 independent dataset (Figure 6), comparison yielded
 384 stable or similar performance, with water-level RMSE of 0.05–0.06 m and NSE of 0.86–0.88,
 385 and H_s RMSE of approximately 0.20 m.

386

387

388



389

390 **Fig 6.** Results of Verification on water level, current, and wave parameters at Station A (left)
 391 and Station B (right) during the second (May 2024) survey campaign

392 It is also noted that wave and current intensities during the calibration period were higher than
 393 those observed during the verification period, which partly explains the slight differences in
 394 error magnitude. Also, the discrepancies between Observed (Oi) and simulated (Si) values for
 395 the both, calibration and verification cases, may be attributed to (i) measurement uncertainty
 396 and short-lived variability in the surf zone and (ii) nearshore modelling limitations, including
 397 sensitivity to offshore forcing, local bathymetry, and SWAN surf-zone parameterizations
 398 (breaking/whitcapping/bottom friction), which particularly affect peak Hs (see Section 4.2).
 399 Overall, the comparable verification skill without retuning confirms that the selected
 400 configuration is physically consistent and not driven by case-specific tuning, providing a
 401 reliable basis for subsequent scenario simulations and morphodynamic analyses.
 402

403 3. Hydrodynamic Simulation of the My Khe Coastal Area

404

405 3.1 Simulation Scenarios

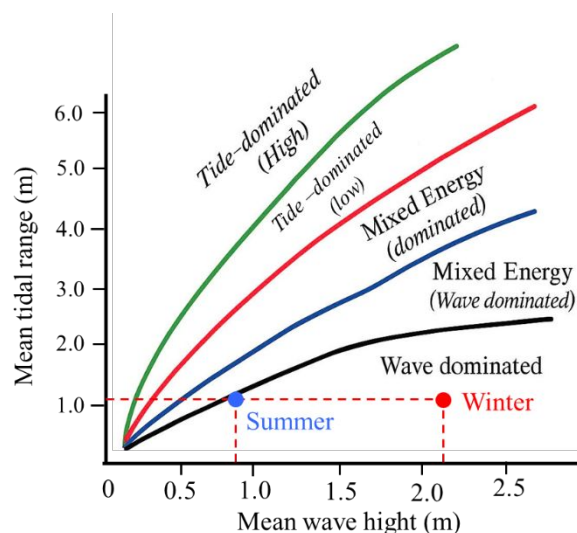
406

407 A detailed analysis of multi-year wave data from 2000 to 2023 for the Da Nang coastal region
 408 provides a robust characterization of the nearshore wave climate relevant to the My Khe
 409 shoreline. For regime interpretation and scenario design, the long-term record was partitioned
 410 into monsoon-controlled seasons and dominant incident directional sectors consistent with the
 411 discrete model forcing directions (Table 2): winter NE (Dir = 45°) and ENE (Dir = 60°), and
 412 summer ESE (Dir = 135°) and SE (Dir = 150°). Seasonal representative significant wave heights

413 (H_s) were defined using the central tendency (mean/median band) of each seasonal H_s
 414 distribution, yielding 0.8–0.9 m for summer and 2.1–2.2 m for winter; these narrow ranges
 415 reflect interannual variability while remaining representative of typical seasonal (background)
 416 forcing used for regime characterization.

417 The coastal environment is mainly characterized by a mixed tidal regime, predominantly
 418 semi-diurnal, having an average tidal range of about 1.2 meters. Such tidal characteristics are
 419 consistent with regional observations reported in prior studies (e.g., Tran et al., 2015). The
 420 dynamic interaction between wave and tidal processes at My Khe beach is illustrated in Figure
 421 8, highlighting the temporal variability and relative contributions of these hydrodynamic forces.

422 According to the coastal classification scheme based on wave–tide interactions developed
 423 by Hayes (1979), coastal environments can be categorized into tide-dominated, wave-
 424 dominated, or mixed regimes depending on the relative energy contributions of waves and tides.
 425 Applying this framework to the My Khe beach area indicates a predominantly wave-dominated
 426 regime, especially during monsoonal seasons (Figure 7). This wave dominance is more
 427 particularly pronounced during the winter northeast (NE) and east-northeast (ENE) monsoon
 428 periods, when prevailing winds and swell conditions intensify wave energy impacting the
 429 shoreline (Nguyen & Pham, 2020). Such seasonal variability in hydrodynamic forcing has
 430 significant implications for coastal sediment transport, shoreline morphology, and erosion
 431 patterns in the region.



432

433

434

435

Fig 7. Seasonal representative H_s values (summer: 0.8–0.9 m; winter: 2.1–2.2 m) from the 2000–2023 record by monsoon-season and directional-sector partitioning and taking the central tendency of each seasonal H_s distribution; ranges indicate interannual variability.

436

437

438

439

440

441

442

Based on the multi-year deep-water (offshore) wave statistics compiled for 2000–2023 for the My Khe coastal area, the previously validated numerical hydrodynamic model was applied to investigate a range of representative climatic scenarios. The two tidal simulation windows selected for winter and summer correspond to the periods used to validate the model's season-specific tidal parameters, based on observed water-level records collected during the January (winter) and May (summer) field campaigns. Wave scenarios (Table 2) were designed to span representative seasonal sea states within the dominant directional sectors adopted in the model.

443

444

445

The multi-year deep-water wave statistics (2000–2023) indicate a pronounced directional concentration within the eastern sector, with ENE dominating (36.89%), followed by SE (18.17%), NE (12.17%), E (10.88%), and ESE (10.87%), whereas all remaining directions

446 occur much less frequently (<3% each). In terms of wave-height distribution, the most common
 447 conditions are $H_s = 0.51\text{--}1.0$ m (37.73%) and $H_s = 1.01\text{--}2.0$ m (32.63%), followed by $H_s < 0.5$
 448 m (16.12%) and $H_s = 2.01\text{--}3.0$ m (11.22%); wave heights exceeding 3.0 m are rare (3.01–4.0
 449 m: 2.05%; 4.01–15 m: 0.25%).

450 A calm-condition case (KB13) was included as a reference baseline. This calm case provides a
 451 “tide-only” benchmark to isolate and quantify wave-driven contributions (e.g., wave-induced
 452 setup and currents) relative to tidally driven hydrodynamics. The complete set of scenarios used
 453 for subsequent analyses is summarized in Table 2, providing an overview of the hydrodynamic
 454 boundary conditions applied in the simulations.

455 **Table 2.** Hydrodynamic simulation scenarios for the Da Nang coastal area

Scénarios	Tidal simulation period	Period of influence	Parameters	Frequency (%)
KB1	16/01/2024–23/01/2024	NE-sector waves (winter)	$H_s=2,5$ m; $T_p=8,0$ s; $Dir=45^\circ$	4,13
KB2	16/01/2024–23/01/2024	NE-sector waves (winter)	$H_s = 2.0$ m; $T_p = 8.0$ s; $Dir = 45^\circ$	4,40
KB3	16/01/2024–23/01/2024	NE-sector waves (winter)	$H_s=1,0$ m; $T_p=6,0$ s; $Dir=45^\circ$	1,91
KB4	16/01/2024–23/01/2024	ENE-sector waves (winter)	$H_s=2,0$ m; $T_p=6,0$ s; $Dir=60^\circ$	19,84
KB5	16/01/2024–23/01/2024	ENE-sector waves (winter)	$H_s=2,5$ m; $T_p=8,0$ s; $Dir=60^\circ$	5,87
KB6	16/01/2024–23/01/2024	ENE-sector waves (winter)	$H_s=1,0$ m; $T_p=6,0$ s; $Dir=60^\circ$	9,30
KB7	16/01/2024–23/01/2024	E-sector waves (winter)	$H_s=1,5$ m; $T_p=6,0$ s; $Dir=90^\circ$	2,29
KB8	16/01/2024–23/01/2024	E-sector waves (winter)	$H_s=1,0$ m; $T_p=6,0$ s; $Dir=90^\circ$	6,28
KB9	15/05/2024–21/05/2024	ESE-sector waves (summer)	$H_s=1,5$ m; $T_p=6,0$ s; $Dir=135^\circ$	1,30
KB10	15/05/2024–21/05/2024	ESE-sector waves (summer)	$H_s=1,0$ m; $T_p=6,0$ s; $Dir=135^\circ$	5,82
KB11	15/05/2024–21/05/2024	SE-sector waves (summer)	$H_s=1,5$ m; $T_p=6,0$ s; $Dir=150^\circ$	1,96
KB12	15/05/2024–21/05/2024	SE-sector waves (summer)	$H_s=1,0$ m; $T_p=6,0$ s; $Dir=150^\circ$	10,33
KB13	15/05/2024–21/05/2024	Calm (tide-only baseline)	Calm conditions	16,12
Other conditions	—	—	Remaining Dir– H_s classes	10,45

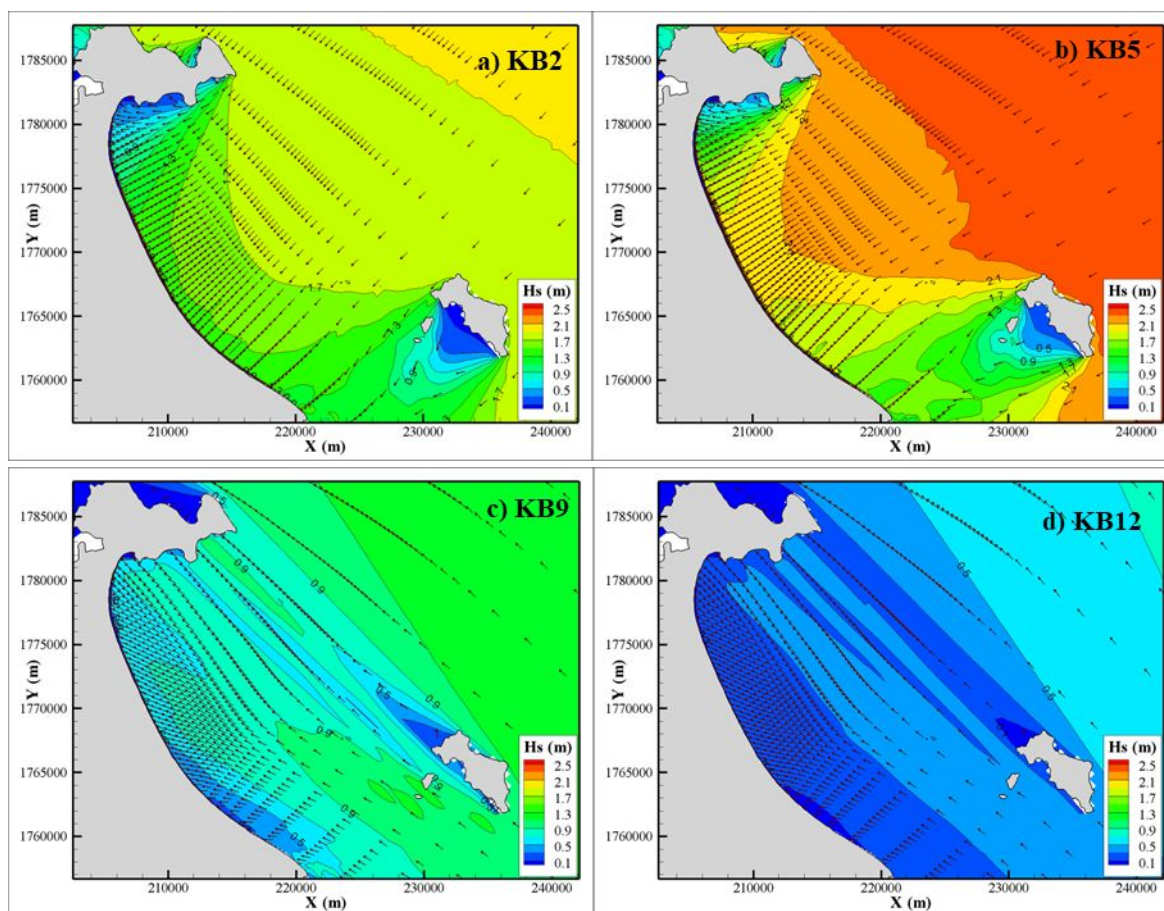
456

457 3.2 Nearshore Wave Characteristics

458 Northeast Monsoon Period

459 Figure 8 (a,b) presents the simulated wave field in the My Khe coastal zone associated with the
 460 northeast (NE) monsoon season. The numerical wave model captures the spatial variability of
 461 wave propagation induced by the complex coastal morphology, particularly the strong
 462 curvature of the shoreline near the Son Tra Peninsula and the Cu Lao Cham Island. This
 463 morphological system, the peninsula and the island, explains the convergence effect of wave
 464 rays during NE monsoon, or the focalization of wave energy hitting the My Khe beach. The

465 alongshore wave-induced currents are intensified and increase the capacity for sediment
 466 mobilization and redistribution along the shore.



467
 468 **Fig 8.** Simulated wave fields in the My Khe beach area at selected times illustrating the
 469 characteristic spatial patterns and propagation directions under (a, b) northeast monsoon wave
 470 conditions (scenarios KB5 and KB2, respectively) and (c, d) southern monsoon wave conditions
 471 (scenarios KB9 and KB12, respectively).

472

473 The convergence effect of waves together with the presence of sheltered zones behind peninsula
 474 and island amplifies sediment transport gradients, which in turn exacerbates erosion phenomena
 475 within embayed coastal sectors (Tsabaris et al. (2025)). In this case, field observations indicate
 476 that these processes conduct the formation and amplification of megacusp (Tanaka et al. 2016,
 477 2017). The simulated wave field also indicates that offshore waves approaching the Son Tra
 478 Peninsula under NE and east-northeast (ENE) wave scenarios consistently refract and propagate
 479 shoreward, reinforcing the wave energy flux directed toward the coastline. The wave directional
 480 pattern generated by the coastal geometry during the NE or ENE monsoon is the dominant
 481 explanation for the spatial patterns with mega cusps observed in the region.

482 These findings align with established coastal morphodynamic principles, whereby wave
 483 convergence zones are hotspots for intensified hydrodynamic forcing and sediment
 484 redistribution (Komar, 1998; Masselink & Hughes, 2003). Understanding these interactions is
 485 essential for predicting shoreline evolution and informing coastal management strategies aimed
 486 at mitigating erosion risks along the My Khe coast.

487 Southwest Monsoon Period

488 Contrary to the higher-energy wave regime associated with the winter northeast monsoon, the
489 summer monsoon wave climate coming from the southeast sector presents significantly lower
490 energy levels along the My Khe shoreline (Figure 8 c,d). Specifically, waves arriving from the
491 east-southeast (ESE) and south (S) directions are strongly attenuated due to the sheltering effect
492 of Island. The latter acts as a natural barrier, protecting the coastline by reducing the nearshore
493 significant wave heights below 0.5 meters.

494 These relatively calm swell conditions promote sediment deposition, leading to net accretion
495 which is observed by beach widening within embayed areas. This sediment accumulation tends
496 to diminish the amplitude of mega cusps features and contributes to the overall stabilization of
497 the My Khe coastal zone. Such seasonal variability in wave energy and sediment dynamics
498 highlights the critical role of local geomorphological features in modulating coastal processes
499 (e.g., Wright & Short, 1984; Masselink & Hughes, 2003).

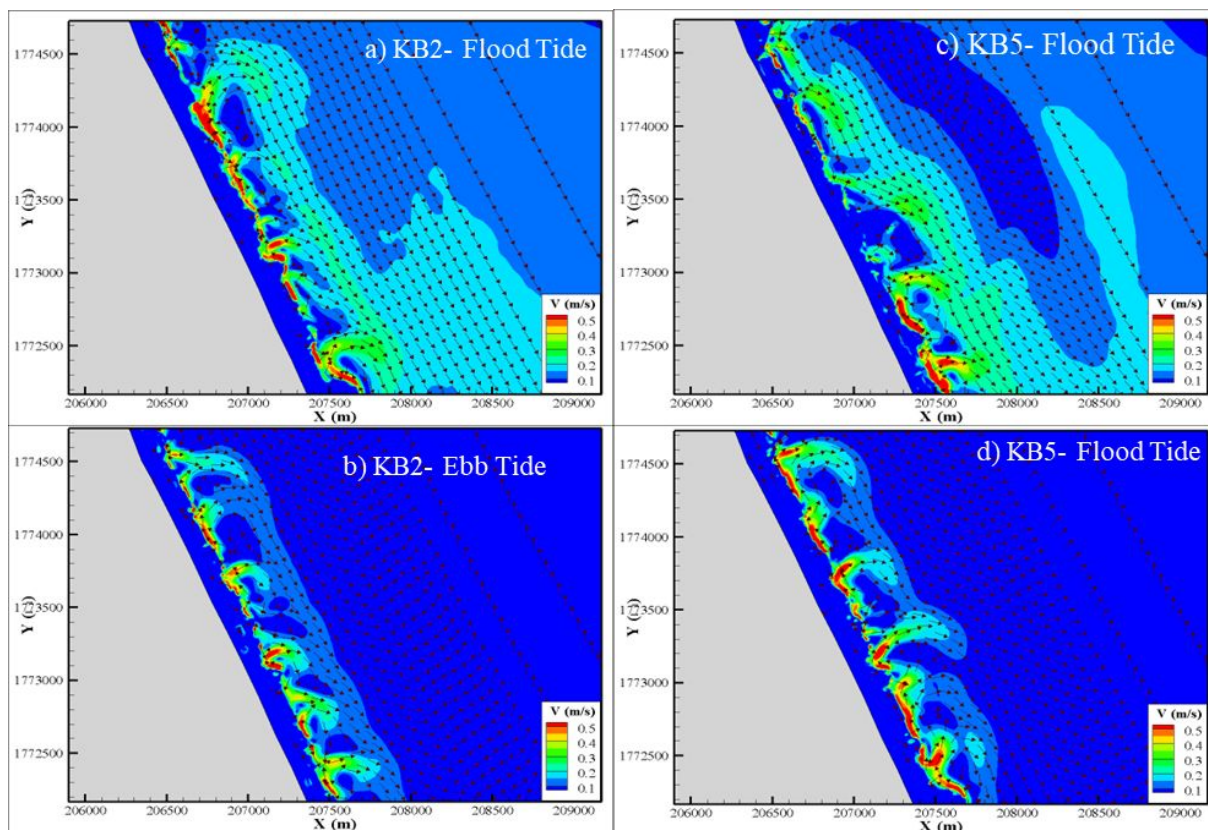
500 **3.3 Nearshore Current Patterns**

501

502 Figure 9 presents the simulated current field in the My Khe coastal area under the influence of
503 wave conditions during the northeast monsoon. Within a 500-meter nearshore zone, wave-
504 induced currents dominate with high intensity, flowing seaward during both flood and ebb tidal
505 phases.

506 During flood tide, wave-driven currents exhibit high velocities, reaching up to 0.45 m/s, and
507 are concentrated primarily near the shoreline. These currents transport sediment offshore and
508 generate strong longshore movement, contributing significantly to coastal morphological
509 changes. During ebb tide, the seaward-directed currents also reach velocities of up to 0.45 m/s,
510 further enhancing sediment transport from the beach toward deeper waters.

511 In offshore areas, tidal currents become dominant, but their magnitudes are generally lower
512 - less than 0.2 m/s - and thus have a limited impact on shoreline morphology. Overall, within
513 the 500-meter nearshore zone during the northeast monsoon, wave-induced currents play a
514 dominant role, exerting strong influence on sediment transport and coastal transformation,
515 while tidal currents are more influential further offshore but with weaker intensity.



516

517

Fig 9. Current field in the My Khe coastal area under northeast monsoon (winter) wave conditions: (a,c) KB2 conditions; (b,d) KB5 conditions.

518

519

520

521

522

523

524

525

526

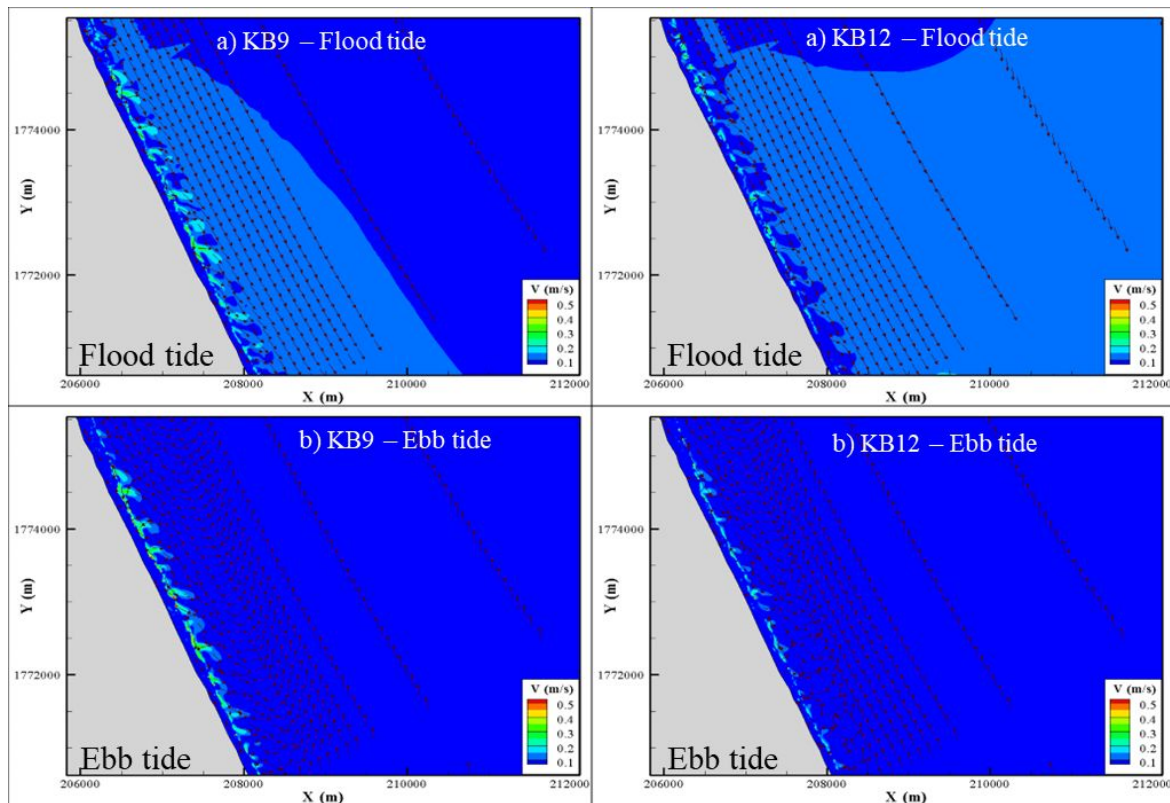
527

528

529

Figure 10 illustrates the velocity field in the My Khe coastal area under the influence of wave conditions during the southwest monsoon. Compared to the northeast monsoon, nearshore current intensity is significantly reduced, reflecting a marked shift in the region's hydrodynamic processes. Nearshore currents exhibit low velocities, generally below 0.2 m/s, and the previously prominent seaward-directed flows are no longer clearly observed—contrasting strongly with the northeast monsoon period, when strong offshore-directed currents were evident.

The reduction in wave energy during the southwest monsoon is a key factor, as it substantially diminishes wave impacts on the nearshore zone. This leads to weakened current activity and limited sediment transport offshore.



530

531

532

533

534

535

536

537

538

539

540

541

542

543

544

545

546

547

548

549

550

551

552

553

554

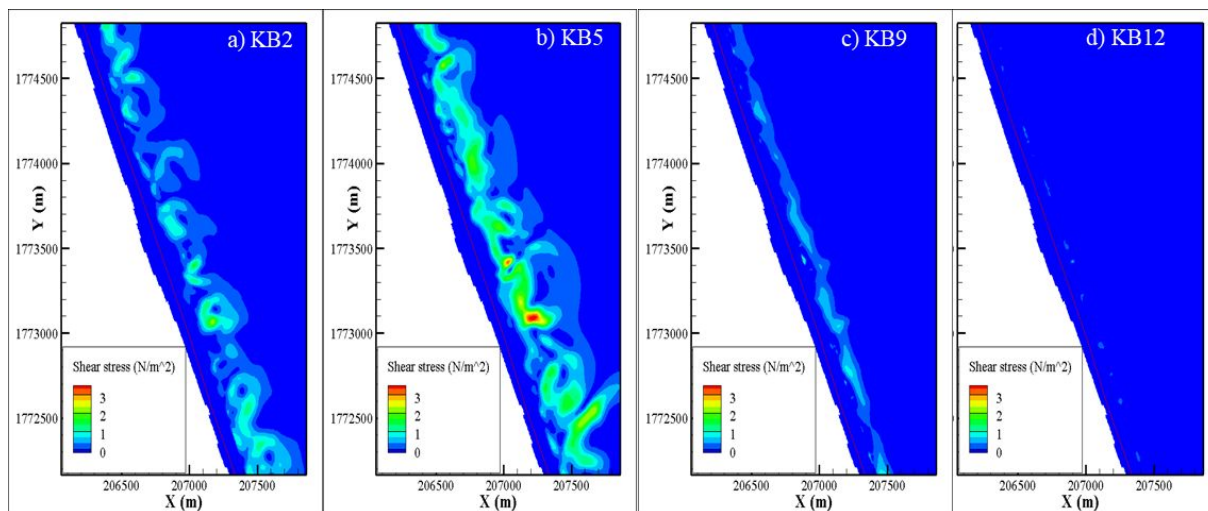
Fig. 10. Velocity field in the My Khe coastal area under southwest monsoon (summer) wave conditions: (a, c) KB9 conditions; (b, d) KB12 conditions

This phenomenon helps explain why mega cusps features are less pronounced during the southwest monsoon - the cusp amplitudes are smoothed, and the troughs are infilled by hydrodynamic weaker conditions - compared to the northeast monsoon. The contrasting impacts of the two monsoon seasons on My Khe Beach highlight that the southwest monsoon induces minimal morphological changes, thereby contributing to shoreline stability and reducing the risk of erosion caused by strong wave and current forces.

3.4 Nearshore bed shear stress Distribution

The My Khe beach area in Vietnam is characterized by notable geographical and climatic features, particularly with strong wave action, especially during the winter months (Figure 11a-b). In winter, bed shear stress increases significantly, with certain areas recording bed shear stress (τ_b) levels up to 4 N/m². This reflects the higher wave energy and current strength prevalent during winter, resulting in considerable bed disruption, sediment movement, and beach erosion. Winter at My Khe is marked by more intense wave action, causing important changes to the beach morphology, altering seabed structure, and influencing sedimentation processes. These changes are critical factors to consider in coastal protection studies and resource management, aimed at developing strategies to mitigate the impacts of climate change and the seasonal dynamics affecting seabed processes.

In contrast, during the summer (Figure 11c-d), bed shear stress remains lower and more evenly distributed, typically ranging from 1 to 2 N/m², and becomes nearly negligible under the mildest case (Figure 11d). This reflects more stable wave and current conditions in summer, with less intense wave energy and current strength compared to winter.



555
 556 **Fig 11.** Numerically simulated nearshore bed shear stress τ_b (N/m^2) under representative winter
 557 (a–b) and summer (c–d) wave conditions: (a) KB2: $H_s = 2.0$ m, $T_p = 8.0$ s, $\text{Dir} = 45^\circ$; (b) KB5:
 558 $H_s = 2.5$ m, $T_p = 8.0$ s, $\text{Dir} = 60^\circ$; (c) KB9: $H_s = 1.5$ m, $T_p = 6.0$ s, $\text{Dir} = 135^\circ$; (d) KB12: H_s
 559 $= 1.0$ m, $T_p = 6.0$ s, $\text{Dir} = 150^\circ$.

560

561 Although summer still experiences wave action, the intensity is significantly lower
 562 compared to winter. The differences in bed shear stress between winter and summer are crucial
 563 for understanding the dynamic processes at My Khe beach.

564 4. Discussions

565 4.1 Monsoon-driven Hydrodynamic (/Morphodynamic) behavior

566 The seasonal monsoon system exerts a dominant influence on wave characteristics along the
 567 My Khe coastline. During the ENE monsoon (winter), waves typically approach the shore with
 568 higher energy and a more perpendicular angle of incidence. Significant wave heights during
 569 this period often range from 1.5 to 2 meters, generating strong longshore and return currents
 570 that enhance offshore sediment transport and promote erosional processes, particularly in
 571 embayed or concave shoreline segments. In contrast, the ESE monsoon (summer) is
 572 characterized by lower wave heights (around 1 meter) and a more oblique angle of wave
 573 approach. These conditions reduce the energy flux toward the shore and favor sediment
 574 deposition, leading to the smoothing or even disappearance of mega cusps features and
 575 contributing to beach accretion.

576 The presence of Cu Lao Cham Island plays a critical role in modulating wave energy
 577 distribution along the coast through a natural wave sheltering effect. During the ENE monsoon,
 578 the island creates a localized sheltered zone due to the quasi-normal wave incidence, resulting
 579 in a diffraction pattern similar to that produced by a detached breakwater. This leads to the
 580 formation of tombolo-like or mega cusps features in the onshore direction. Conversely, during
 581 the ESE monsoon, the oblique wave approach results in a broader and more continuous
 582 sheltered zone that extends across much of My Khe Beach. This extensive protection reduces
 583 wave energy exposure and enhances sediment accumulation, particularly in the central and
 584 southern sections of the beach.

585 Bed shear stress is a key parameter in determining sediment mobilization and transport. The
 586 numerical simulations reveal a clear seasonal contrast in bed shear stress patterns. During the
 587 ENE monsoon, elevated wave energy and stronger longshore currents generate higher bed shear
 588 stress values, particularly in exposed zones, which facilitates sediment erosion and the
 589 development of megacusps. In contrast, the ESE monsoon is associated with lower current
 590 velocities and reduced bed shear stress, especially in the sheltered zones. These conditions favor
 591 sediment deposition and embayment infilling, contributing to the seasonal expansion of the
 592 beach profile. The spatial variability in bed shear stress, driven by both wave direction and

593 sheltering effects, underscores the complex interplay between hydrodynamic forcing and
594 morphological response.

595 At the same time, these bed shear stress estimates must be interpreted with caution. They are
596 influenced by spatial resolution (bathymetric smoothing, Manning or bottom-friction
597 parameterization) and by temporal resolution constraints imposed by the CFL condition. At
598 meter-scale resolution, sub-grid variability in roughness and turbulence cannot be explicitly
599 resolved, and bed shear stress should therefore be regarded as an effective, bulk indicator of
600 hydrodynamic forcing rather than a point-scale representation of near-bed processes.

601

602 **4.2 Implications and Limitations**

603 This study highlights how seasonal monsoon forcing controls the formation and decay of mega-
604 cusps at My Khe Beach, providing information of direct relevance to coastal planning and
605 management. Understanding the timing and magnitude of seasonal erosion and accretion is
606 essential for designing adaptive, climate-resilient coastal protection measures and for
607 anticipating future shoreline change.

608 The validated Delft3D model reproduced the local hydrodynamic conditions with good
609 accuracy and revealed a clear relationship between wave energy and seaward-directed return
610 currents. During the ENE monsoon, high-energy waves ($H_s \approx 1.5\text{--}2$ m) and strong north-to-
611 south longshore currents (up to 0.45 m s^{-1}) intensify offshore sediment transport, deepening the
612 embayments of mega-cusps and promoting erosion. Conversely, the calmer ESE monsoon (H_s
613 ≈ 1 m; longshore currents < 0.2 m s^{-1}) favors onshore sediment transport and the partial
614 smoothing or erasure of cusp morphology.

615 These seasonal contrasts generate a cyclic pattern of erosion and recovery and a non-
616 equilibrated, hysteretic shoreline response, resulting in a long-term erosional trend.
617 Such insights are valuable for hazard mitigation and nourishment planning, as they identify
618 periods of heightened vulnerability and potential windows for beach recovery.

619 The presence of Cu Lao Cham Island further modulates wave energy, acting as a natural
620 detached breakwater. During the ENE monsoon the island produces a narrow, quasi-normal
621 wave-sheltered zone that encourages the development of tombolo-like features and mega-cusps.
622 In summer, when waves arrive at a more oblique angle, the sheltered zone broadens and
623 promotes wider beach accretion. Recognising these sheltering effects is critical for designing
624 future coastal structures and for predicting the spatial variability of erosion risk along My Khe
625 Beach.

626 Despite these advances, several constraints should be noticed. First, storm-surge events were
627 not explicitly modelled in the current study. Although Typhoon Noru (2023) produced
628 significant morphological change, the lack of high-resolution observations during such extreme
629 events limits our ability to quantify their contribution to sediment transport and shoreline
630 adjustment. Future research should integrate storm-surge scenarios through targeted field
631 campaigns, remote sensing, or hindcast modelling.

632 Second, the analysis is limited by the availability of bathymetric data. Surveys were conducted
633 in January 2023 and January 2025, with only a single intermediate dataset in May 2024. This
634 restricts the model's ability to capture intra-annual morphological change and limits the
635 temporal resolution of seasonal variability. Although the relatively low hydrodynamic energy
636 during the study period lessens the likelihood of major short-term morphological adjustments -
637 making the use of a static bathymetry acceptable for model verification - more frequent
638 bathymetric monitoring would greatly enhance confidence in long-term trend assessments.

639 Third, the results should be interpreted in light of the inherent limitations of the modeling
640 framework. The Delft3D setup is based on depth-averaged shallow-water equations, which
641 provide an efficient and robust representation of large-scale nearshore hydrodynamics but
642 necessarily rely on parameterizations to represent highly complex physical processes. In
643 particular, nearshore bed shear stress is strongly influenced by turbulence generated by wave
644 breaking, swash-surf interactions, and strong vertical velocity gradients. These processes

645 involve non-hydrostatic pressure distributions, pronounced nonlinearities, large wave
646 steepness, and intense energy dissipation, which are only partially captured within a hydrostatic,
647 depth-averaged formulation.
648

649 **5. Conclusion and perspectives**

650 This study demonstrates how the seasonal monsoon regime and the sheltering effect of Cu Lao
651 Cham Island jointly govern the lifecycle (formation, evolution, and decay) of mega-cusps at
652 My Khe Beach. Based on satellite and field observations, a numerical (Delft3D) model has been
653 validated revealing a cyclical pattern of wintertime erosion and summertime recovery,
654 reflecting the interaction between high-energy northeast monsoon waves and calmer southwest
655 monsoon conditions.

656 These findings emphasize that shoreline changes in monsoon-dominated settings are
657 strongly non-linear and spatially variable, highlighting the need for site-specific monitoring and
658 adaptive management. While the present work focused on seasonal variability of flow dynamic
659 under typical conditions, the next step is to extend modelling to extreme events and higher-
660 resolution bathymetric datasets, in order to better quantify the role of storms and short-term
661 morphological adjustments.

662 By clarifying the seasonal mechanisms and highlighting knowledge gaps, this research
663 provides a robust foundation for future coastal protection strategies and for refined numerical
664 studies of sediment dynamics in coastal systems influenced by storm surges, cyclonic activity,
665 monsoons, and both tropical and extra-tropical climatic scenarios.
666

667 Building on these findings, future work will aim to better distinguish the respective roles of
668 wave height and wave direction in driving erosion and deposition processes during the ENE
669 and ESE monsoon seasons. This will involve a more detailed examination of sediment transport
670 dynamics, including how variations in wave energy and incident angles influence sediment
671 pathways and morphological responses along the My Khe shoreline.

672 A long-term perspective will also be adopted by incorporating multi-seasonal and pluri-
673 annual datasets. This approach will help identify persistent trends and interannual variability in
674 coastal evolution, offering a more robust understanding of the cumulative effects of seasonal
675 forcing on shoreline stability.

676 In addition, the study will explore the impact of extreme wave conditions, which were
677 discussed in the current work's discussion section. While field measurements during such high-
678 energy events pose significant risks, the validated numerical model provides a valuable tool for
679 simulating and predicting sediment behavior under these extreme scenarios. This predictive
680 capability is essential for proactive coastal management and hazard mitigation.

681 To further validate model outputs and improve the accuracy of erosion and accretion zone
682 identification, future work may also incorporate sediment tracing techniques. Specifically,
683 methods based on the mapping of sediment-associated radionuclides could be employed. Given
684 the contrasting energy environments along My Khe Beach—ranging from sheltered zones with
685 low wave energy to highly exposed areas—this site presents promising conditions for applying
686 such techniques to validate sediment deposition and erosion patterns. In parallel, a more
687 detailed quantification of absolute bed shear stress, including extended sensitivity analyses and
688 higher-order process representation, will also be addressed in future studies to strengthen
689 understanding of the links between hydrodynamic forcing and morphological response.
690

691 **Acknowledgements**

692 This research was supported by the National-Level Applied Research and Technology
693 Development Project titled *“Development of model systems to assess and forecast*

694 *morphological changes and countermeasures to stabilize the beaches in the Mid-Central*
695 *Vietnam region*” project, funded by the Ministry of Science and Technology, Vietnam, code:
696 42/22-ĐTĐL.CN-XNT. The financial support for travel costs provided by Quebec Ministry of
697 International Relations and Francophonie, MRIF, is gratefully acknowledged MRIF-Quebec-
698 Vietnam (Project name: RESALECC, 2023-25).
699

700 **Competing interests**

701 No competing interest for all authors.

702

703 **Data availability**

704 Data are available upon reasonable request.

705

706 **References**

- 707 Castelle, B., Scott, T., Brander, R. W., & McCarroll, R. J. (2016). Rip current types,
708 circulation and hazard. *Earth Science Reviews*, 163, 1–21.
- 709 Clark (1997). Coastal zone management for the new century. *Ocean & Coastal*
710 *Management*, Vol. 37, No. 2: 191-216.
- 711 Chowdhury, P., Goud, L. N. K., Susana, L., Kumar, S. J., & Ranjan, B. M. (2023). Climate
712 change and coastal morphodynamics: Interactions on regional scales. *Science of The*
713 *Total Environment*, 887, 164542. <https://doi.org/10.1016/j.scitotenv.2023.164542>
- 714 Craig-Smith, S. J. (2021). Cuspate Forelands. In C. W. Finkl & C. Makowski (Eds.),
715 *Encyclopedia of Coastal Science* (pp. 672–673). Springer.
716 https://doi.org/10.1007/978-3-319-93806-6_106
- 717 Dien, D.C., Tanaka, H., Viet, N.T., Manh, D.V., 2019. Numerical model for simulating
718 sand terrace formation in front of the Cua Dai River mouth. *Proceedings of the 10th*
719 *Int. Conf. on Asian and Pacific Coasts (APAC 2019)*, doi.org/10.1007/978-981-15-
720 0291-0_81
- 721 Egbert, G.D. and Erofeeva, S.Y., 2002. Efficient inverse modeling of barotropic ocean
722 tides. *Journal of Atmospheric and Oceanic technology*, 19(2), pp.183-204.
- 723 Guza, R. T., & Inman, D. L. (1975). Edge waves and beach cusps. *Journal of Geophysical*
724 *Research*, 80(21), 2997–3012.
- 725 Hayes M.O. (1979). Barrier Island Morphology as a function of Tidal and Wave Regime.
726 In *Barrier Islands from the Gulf of St. Lawrence to the Gulf of Mexico* (pp. 1–27).
727 New York: Academic Press.
- 728 Hue, N.H., Thanh, N.H. (2020). Assessing the Impact of Massive Development of Beach
729 Resorts on Current Status of Coastal Erosion Along the Central Coast of Vietnam. In:
730 Viet, N.T, Xiping, D., Thanh Tung, T. (eds) APAC 2019. APAC 2019. Springer,
731 Singapore. https://doi.org/10.1007/978-981-15-0291-0_76
- 732 IPCC (2023). Sixth Assessment Report. *Climate Change 2023: Impacts, Adaptation and*
733 *Vulnerability*
- 734 Komar, P. D. (1998). *Beach Processes and Sedimentation* (3rd ed.). Prentice Hall
- 735 Kulp, S., & Strauss, B. (2019). Coastal population exposure to sea-level rise and flooding.
736 *Nature Communications*, 10, 4844.
- 737 Lesser, G. R., Roelvink, J. A., van Kester, J. A. T. M., & Stelling, G. S. (2004).
738 Development and validation of a three-dimensional morphological model. *Coastal*
739 *Engineering*, 51(8), 883–915. <https://doi.org/10.1016/j.coastaleng.2004.07.014>
- 740 Martinez, G., Bizikova, L., Blobel, D., Swart, R. (2011). Emerging Climate Change Coastal
741 Adaptation Strategies and Case Studies Around the World. In: Schernewski, G.,

- 742 Hofstede, J., Neumann, T. (eds) *Global Change and Baltic Coastal Zones*. Coastal
743 Research Library, vol 1. Springer, Dordrecht. [https://doi.org/10.1007/978-94-007-](https://doi.org/10.1007/978-94-007-0400-8_15)
744 [0400-8_15](https://doi.org/10.1007/978-94-007-0400-8_15)
- 745 Masselink, G., & Hughes, M. G. (2003). *Introduction to Coastal Processes and*
746 *Geomorphology*. Hodder Arnold.
- 747 Morales, J.A. (2022). Mitigation, Coastal Policies and Integrated Coastal Zone
748 Management. In: *Coastal Geology*. Springer Textbooks in Earth Sciences,
749 Geography and Environment. Springer, Cham. [https://doi.org/10.1007/978-3-030-](https://doi.org/10.1007/978-3-030-96121-3_30)
750 [96121-3_30](https://doi.org/10.1007/978-3-030-96121-3_30)
- 751 Nielsen, P. (1992). *Coastal Bottom Boundary Layers and Sediment Transport*. World
752 Scientific.
- 753 Nguyen, T. H., & Pham, V. T. (2020). Seasonal wave climate and its impact on coastal
754 erosion along central Vietnam. *Journal of Coastal Research*, 36(2), 345–357.
755 <https://doi.org/10.2112/JCOASTRES-D-19-00123.1>
- 756 Viet. N.T., Tanaka, H., Tinh, N. X., Duy, D. V., & Luc, N. V. (2018). *Recent Shoreline*
757 *Retreat of My Khe Beach, Da Nang, Central Vietnam*. Proceedings of the 8th
758 International Conference on Fluid Mechanics (ICFM8), Tohoku University, Sendai,
759 Japan.
- 760 Thanh T.M., Tanaka H., Mitobe Y., Viet N.T., and Almar R., 2018. Seasonal Variation of
761 Morphology and Sediment Movement on Nha Trang Coast, Vietnam. *Journal of*
762 *Coastal Research* SI 81, pp 22–31, DOI: 10.2112/SI81-004.1
- 763 Tinh. N.X, Tanaka, H., Viet, N. T., Zviely, D., Luc, N. V., Duy, D. V., & Huy, T. D. (2018).
764 Investigation of mega-cusp formation causing coastal erosion in Vietnam.
765 *Proceedings of the 8th International Conference on Fluid Mechanics (ICFM8)*.
766 International Conference on Fluid Mechanics, Tohoku University, Sendai, Japan.
- 767 Pang, T., Wang, X., Nawaz, R.A. *et al.* Coastal erosion and climate change: A review on
768 coastal-change process and modeling. *Ambio* 52, 2034–2052 (2023).
769 <https://doi.org/10.1007/s13280-023-01901-9>
- 770 Pugh D., 2004. *Changing sea levels*, Cambridge University Press, ISBN0521532183
- 771 Short, A.D. & Masselink, G. (1992). Embayed and structurally controlled beaches. *Coastal*
772 *Engineering*, 16(1), 173–210.
- 773 Tanaka, H., Hoang, V.C. and Viet, N.T. 2016. “Investigation of morphological change at
774 the Cua Dai river mouth through satellite image analysis”, Proceedings of 35th
775 International Conference on Coastal Engineering.
- 776 Tanaka, H., Duy, D.V. and Viet, N.T. 2017. “Evaluation of longshore sediment transport
777 rate along the Thu Bon River delta coastline in Vietnam”, Proceedings of the 37th
778 IAHR World Congress.
- 779 Thornton, E. B., MacMahan, J., & Sallenger, A. H., Jr. (2007). Rip currents, mega-cusps,
780 and eroding dunes. *Marine Geology*, 240(1–4), 151–167.
- 781 Tran, Q. H., Le, D. T., & Hoang, N. T. (2015). Tidal dynamics and hydrodynamic modeling
782 in the Da Nang coastal region. *Vietnam Journal of Marine Science and Technology*,
783 15(3), 112–123.
- 784 Tsabaris, C.; Tejera, A.; Koomans, R.L.; Pham van Bang, D.; Hammouti, A.; Malliouri, D.;
785 Kapsimalis, V.; Martel, P.; Arriola-Velásquez, A.C.; Alexakis, S.; et al. Evaluation
786 of Coastal Sediment Dynamics Utilizing Natural Radionuclides and Validated In-Situ
787 Radioanalytical Methods at Legrena Beach, Attica Region, Greece. *J. Mar. Sci. Eng.*
788 **2025**, 13, 1229. <https://doi.org/10.3390/jmse13071229>
- 789 Viet, N.T., Tanaka, H., Tinh, N. X., Duy, D. V., & Luc, N. V. (2025). *Recent Shoreline*
790 *Retreat of My Khe Beach, Da Nang, Central Vietnam*. Intern. Report.
- 791 Viet, N.T., Hoang, V.C., Hai, H.D., Duy, D.V., Giap, N.V., and Tanaka, H. 2015. “Analysis
792 on erosion of beach adjacent to the Cua Dai River mouth, central Vietnam”,
793 Proceedings of 5th International Conference on Estuaries and Coasts, pp.153-158.

- 794 Vila-Concejo A, Fellowes TE, Gallop S, et al. Morphodynamics and management
795 challenges for beaches in modified estuaries and bays. *Cambridge Prisms: Coastal*
796 *Futures*. 2024;2:e11. <https://doi:10.1017/cft.2024.7>
- 797 Williams, J. J., & Esteves, L. S. (2017). Guidance on Setup, Calibration, and Validation of
798 Hydrodynamic, Wave, and Sediment Models for Shelf Seas and Estuaries. *Advances*
799 *in Civil Engineering*, 2017, 1–25. <https://doi.org/10.1155/2017/5251902>.
- 800 Wright, L. D., & Short, A. D. (1984). Morphodynamic variability of surf zones and
801 beaches: A synthesis. *Marine Geology*, 56(1-4), 93–118.
- 802